HEFAT2007
5th International Conference on Heat Transfer, Fluid Mechanics and Thermodynamics
Sun City, South Africa
Paper number: CG1

THREE-DIMENSIONAL SIMULATIONS OF ELECTRONIC MEMORY MODULES COOLING IN NATURAL CONVECTION CONDITIONS

Cammarata G., Petrone G.*, Sorge G.
*Author for correspondence
Department of Industrial and Mechanical Engineering,
University of Catania,
Catania, 95125,
Italy,
E-mail: gpetrone@diim.unict.it

ABSTRACT

Navier-Stokes and energy equations are numerically solved for modelling fluid-dynamical and thermal behaviour of air surrounding horizontally arranged Dual-Inline-Memory-Modules. A complex three-dimensional flow pattern is highlighted, that significantly contributes in heat dissipation of the analysed electronic devices. The present communication contribute, as scientific and technical tool, for investigation on critical cooling conditions for electronic equipment and for innovative projects of fan-less computer architecture.

NOMENCLATURE

C_p	[J/(kg K)]	Isobaric specific heat
$\boldsymbol{g}$	[m/s^2]	Gravity acceleration
$\boldsymbol{I}$	[-]	Identity tensor
k	[W/mK]	Thermal conductivity
Q_{DIMM}	[W]	Power supplied to DIMM
R	[m^{2}K/W]	Interfacial thermal resistance
T	[°C]	Temperature
t	[s]	Time
$\boldsymbol{u}$	[m/s]	Velocity vector (u, v, w)
z	[m]	Cartesian axis direction

Special characters

η	[Pa s]	Dynamical viscosity
ρ	[kg/m^3]	Density
Ω	[m^3]	Volume
Σ	[m$_2$]	Surface

Subscripts

CHIP	CHIP
PCB	Printed Circuit Board

INTRODUCTION

Thermal design of electronic devices is an argument of high scientific, industrial and economic interest because of the primary importance that reliability and performance of these equipments cover in a very wide domain of technological applications. Electronic devices produce heat as a by-product of their normal operation. When electronic devices are not efficiently cooled their lifetime and reliability are dramatically reduced. The reliability and lifetime of semi-conductor components are mainly influenced by thermo-mechanically induced stress and operation temperature, both of which depend on the thermal design [1]. Solder joint reliability is in particular a key aspect of electronic package reliability [2]. Because of periodical thermal loading, solder joints are subjected to fatigue mechanical stresses. In order to assure correct conditions for thermal dissipation of electronic devices during their functioning, several kinds of heat transfer mechanisms are commonly adopted in technological applications, such as natural, mixed or forced convection. The passive character of cooling by natural convection makes it very attractive for application in electronic devices. Cooling of computer boards can be studied by idealizing them as forming horizontal or vertical channels [3]. The buoyancy force due to temperature difference acts on the fluid causing it to flow up through the channel. This is reliable, low cost and maintenance free [4]. Moreover, some of the above discussed components, normally designed for operating in forced convection conditions, commonly operate in off-design mixed or natural convection conditions. In fact, in very wide real operative conditions, cables, drive bays, and brackets can determinate bypass of the forced airflow over the electronic components, forcing the subsystem to operate in natural convection. Therefore, natural convection represents a critical heat transfer mechanism assuring cooling if forced airflow, for any reason, falls down. From a theoretical point of view, cooling of electronic packages has created emphasis on understanding the basic convective fluid flow over discrete heat sources, which have different characteristics from the traditionally studied convection from a heated whole wall [4]. On the other hand, most of the studies in the literature are regarding vertical channels [5, 6, 7] while only few investigations can be found concerning the heat transfer from discrete heat sources inside horizontal channels for air [8,

9]. Recently, the horizontal configuration has taken a particular interest because of the innovative architectures for Dual-Inline-Memory-Modules (DIMM) disposition proposed for Personal Computers by some of their leading constructors [10]. In this study we numerically analyze natural convection heat transfer for DIMM systems, disposed as predicted by a recently proposed form factor. The considered physical system is modelled by horizontal air-filled layers bounded by parallel walls in which multiple heat sources are present. Both transient and steady form of Navier-Stokes and energy equations are numerically solved by using a FEM based software.

PHYSICAL SYSTEM

The actually most used Random Access Memories in Personal Computers are the Dual-Inline-Memory-Modules (DIMM). They are made of 4-16 chip of synchrony dynamical memory with random access (SDRAM), type DDR (Double Data Rate) or DDR2 [11]. Chips are characterized by very small dimensions (i.e. 135x30x1,3 mm) and they are mounted on a Printed Circuit Board (PCB). The PCB disposes of a certain number of PIN both on its top and bottom face. An example of a DIMM is reported in Figure 1. These components are object of the Joint Electron Device Engineering Council (JEDEC) standards [12]. According to JEDEC specifications, the mean parameter indicating thermal performance of DIMM is the total thermal resistance θ_{TOT} between miniaturized integrated circuit and surrounding environment. This represents the sum of sequential thermal resistances, such as junction-package resistance, package-heat sink resistance (if a heat sink is present), heat sink-ambient resistance (Figure 2).

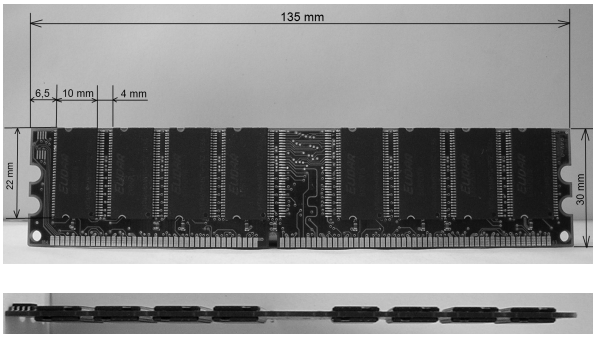

Figure 1 Bottom and backside views of a DIMM module.

By knowing θ_{TOT} value, it is possible, for a chosen ambient temperature $T_{AMBIENT}$ and for a standard active power of 1 [W], analytically evaluating the junction temperature $T_{JUNCTION}$ of the chip. In order to guarantee the reliability of the memory modules, it is strictly necessary that chip does not over, during its functioning, the maximum temperature recommended in the technical documentations of constructors. These values are commonly comprised in the range 80-110 [°C]. For predictive estimation of operative temperature of DIMM, leading constructors recommend computational modelling in spite of analytical determination of temperature by JEDEC indications [13]. In fact analytical determination of $T_{JUNCTION}$ could be not exhaustive because of the lack of consideration of several significant factors, first of all the proximity of other heat sources.

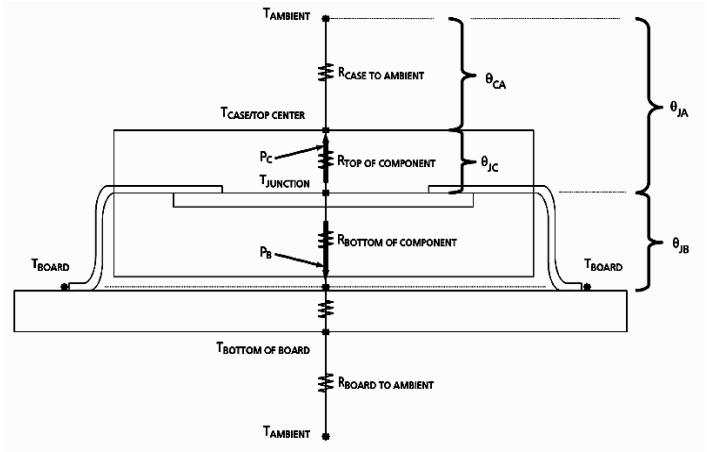

Figure 2 Scheme of a cross section of a chip mounted on a circuit board: primary thermal resistances.

Considering a vertically disposed mainboard (tower configuration for a PC case), according to a recently proposed form factor, DIMM modules are arranged in horizontal disposition, as showed in the top portion of Figure 3. The PCB, where chips are arranged, is perpendicularly connected to the vertical mainboard by specific sockets with lateral guides. DIMM are electronic devices that do not emit energy in the form of radio or electromagnetic waves. On the basis of the conservation law of energy, we can estimate that all the electrical power absorbed by DIMM is then dissipated as thermal power, according to the Joule effect. In order to evaluate the thermal load it is so recommendable to quantify the electrical alimentation power.

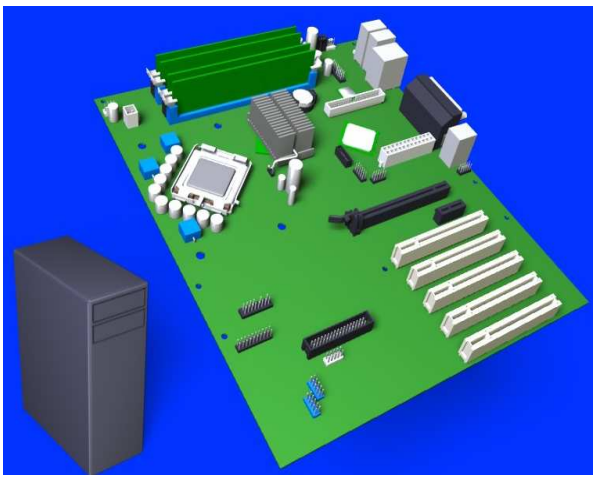

Figure 3 Principal components arranged on a mainboard, according to a recently proposed form factor.

That is given by a basic portion independently absorbed for any operative conditions (related to active and pre-charge states), added by another portion characteristic of the specific operative state, such as activation commands, input/output

operations or writing/reading operations. The total electrical power absorbed by a memory module can be evaluated by specific expression reported in the constructors technical documentation [11, 13].

NUMERICAL MODEL

Let now consider the geometry reported in Figure 4. As shown, a twin set of chips is overlapped on two horizontal circuit boards fixed in their backsides to sockets.

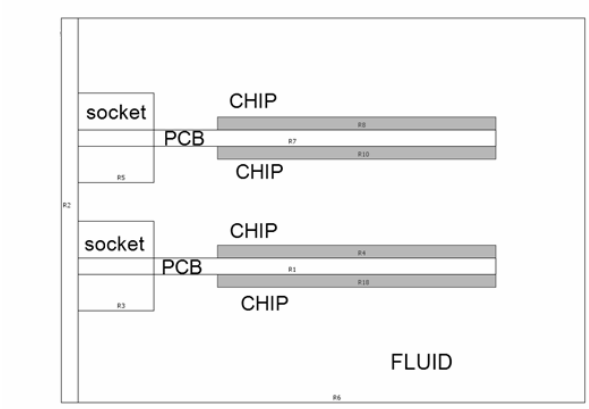

Figure 4 Geometrical scheme of the studied system.

The electronic devices stand in a surrounding air volume. In natural convection, the fluid is propelled by the buoyancy force, generated by a non-uniform density distribution due to local temperature gradients. In the present configuration, heating of fluid is related to the presence of heat sources plunged in the air volume. The physical system is mathematically governed by conservation laws: Navier-Stokes equations, characterizing laminar flow of an incompressible fluid, and energy equation, defining the equilibrium between heat fluxes and heat sources. The governing partial differential equations are reported in following for the different considered domains, respectively:

Fluid:

$$\begin{cases} \rho\dfrac{\partial \mathbf{u}}{\partial t}+\rho(\mathbf{u}\cdot\nabla)\mathbf{u}=\nabla\cdot\left[-p\mathbf{I}+\eta(\nabla\mathbf{u})\right]+(\rho-\rho_0)\mathbf{g} \\ \nabla\cdot(\rho\mathbf{u})=0 \\ \rho C_P\dfrac{\partial T}{\partial t}+\nabla\cdot(-k\nabla T)+\rho C_P\mathbf{u}\cdot\nabla T=0 \end{cases}$$

PCB and sockets:

$$\rho_{PCB}C_{PPCB}\frac{\partial T}{\partial t}+\nabla\cdot(-k_{PCB}\nabla T)=0$$

Chip:

$$\rho_{CHIP}C_{PCHIP}\frac{\partial T}{\partial t}+\nabla\cdot(-k_{CHIP}\nabla T)=\frac{Q_{DIMM}}{n_{CHIP}\cdot\Omega_{CHIP}}$$

Definition of adopted symbols in the above equations are defined in nomenclature. Fluid-dynamical boundary conditions can be qualitatively expressed as:

- No-slip conditions on interfaces between fluid and solid elements;
- Imposed pressure value on the top boundary of the fluid domain;
- Slipping conditions for the velocity vectors on lateral boundaries of the fluid domains (3D models);

while thermal boundary conditions can be resumed as:

- Adiabatic walls for circuit boards and socket;
- Convective heat flux for the top boundary of the fluid domain;
- Imposed temperature (ambient temperature) for the bottom boundary of the fluid domain;

Thermo-physical properties of materials are considered constant for chip (silicon), PCB and sockets (FR4), while density, viscosity and thermal diffusivity of air are expressed as function of temperature. Spatial operators of continuous conservation equations are discretized on no-structured computational meshes, made of triangular (2D) or tetrahedral (3D) elements automatically generated by the used software (COMSOL MultiPhysics, version 3.2). Then, discrete equations, with boundary conditions, are numerically solved by using a direct method (UMFPACK) for linear systems. Computations are carried-out on a 64 bit calculator of 16 GB of RAM.

Validation of Numerical Model

Validation of numerical models has been assured by successfully comparison of test results with experimental data coming from literature. In particular, results of simulation for vertical channels with multiple heat sources plunged in air, have been preliminary compared with those experimentally obtained by Ortega [14]. In Figure 5 we report geometry, thermal and fluid-dynamical fields obtained respectively for 2D and 3D numerical models built in conformity with respect to the system analysed in the reference.

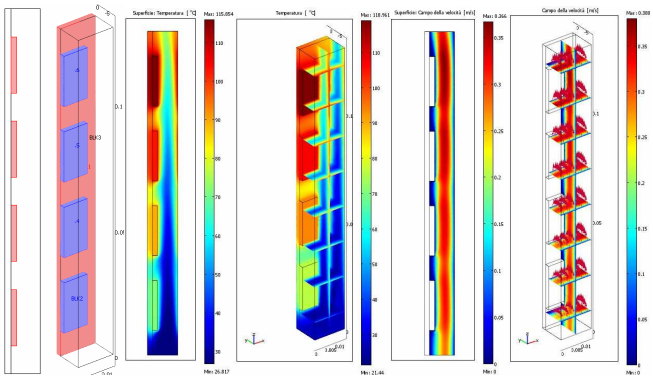

Figure 5 Geometry (2D, 3D), thermal fields (2D, 3D) and velocity fields (2D, 3D) of the numerical model built for validation with experimental results previously published [14].

In these models length of PCB is 0.13 [m], while its thickness is 0.002 [m]. Ambient temperature is set 27 [°C] and heat

sources globally dissipate 1 [W] of power. In Figure 6 thermal transmittance h_{0i} between the *i*-heat source surface (4 surfaces for the presented model) and inlet section for fluid, obtained both for 2D and 3D numerical models, are compared with experimental results of literature [14].

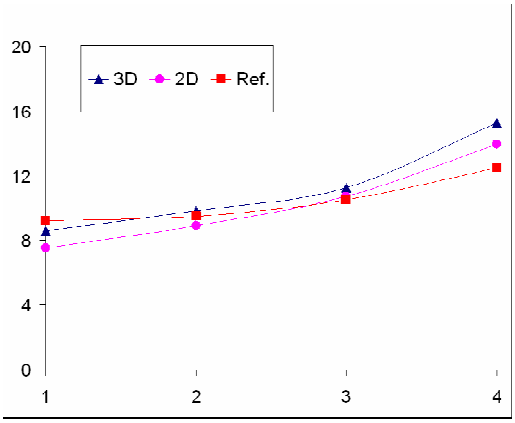

Figure 6 Comparison of thermal transmittance [W/(m2K)] for vertical channels in natural convection conditions between present 2D (circle) and 3D (triangle) numerical results and those experimentally detected in the reference (square) [14].

The compared thermal transmittance is defined as:

$$h_{Oi} = \frac{\frac{1}{\Sigma_1}\int q_i d\Sigma_1}{\frac{1}{\Sigma_2}\int T_{s,i} d\Sigma_2 - T_{f,0}}$$

where Σ_1 and Σ_2 are the total and vertical surface of the heat sources respectively, q_i is the specific thermal flux and $T_{f,0}$ and $T_{s,i}$ are the inlet temperature for fluid and the *i*-vertical surface mean temperature. From Figure 6 a very good agreement between present results and those published in the reference is evident. Remarkable small gaps between present results with respect to reference are probably due to thin difference in geometry of systems.

RESULTS

This section is divided into two subsections. In the first one both transient and steady two-dimensional solutions of Navier-Stokes and energy equations are presented for transversal section of the analysed physical system, while in the second one three-dimensional steady models are discussed.

Transient and steady 2D models

In Figure 7 we report thermal and fluid-dynamical fields for 4 time steps of a transient analysis conducted in a temporal range of 0.1 [s]. System is initialized with rest conditions for fluid, $T_{AMBIENT}$=30 [°C] (t=0 [s]) and a power Q_{DIMM}=0.5 [W] globally supplied to the heat sources. The transient time for the system has been detected to be very short. Fluid, semi-confined by the overlapped solid layers, is quickly propelled by chips heating and forced to flow outside the semi-confined region (t=0.03 [s]). Velocity field assumes a pseudo-parabolic profile, reaching its maximum in correspondence of the middle region between overlapped boards (t=0.07 [s]). At the same time, a convective fluid structure begins to form close to the upper circuit board and backside socket. Then, this structure assumes a defined shape while a second dissipative re-circulating cell appears in the semi-confined region of fluid (t=0.1 [s]). At steady conditions, illustrated by picture in Figure 8, this "internal" re-circulating cell increases, extending over a half about of the semi-confined cavity.

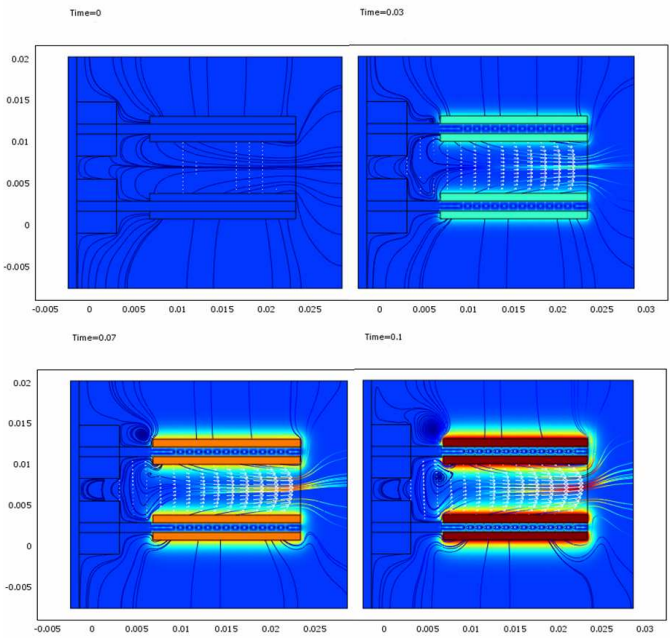

Figure 7 Transient temperature fields, streamlines of flow and velocity vectors for t∈ {0; 0.03; 0.07; 0.1} [s].

Its rotational motion induces arising of a further dissipative "half-roll", standing close to the geometrical end of the solid boards and chips. Generation of counter-rotating convective cells is induced by the onset of thermo-convective instability, certainly amplified both by adherence conditions at boundaries and geometrical singularity in the cavity shape.

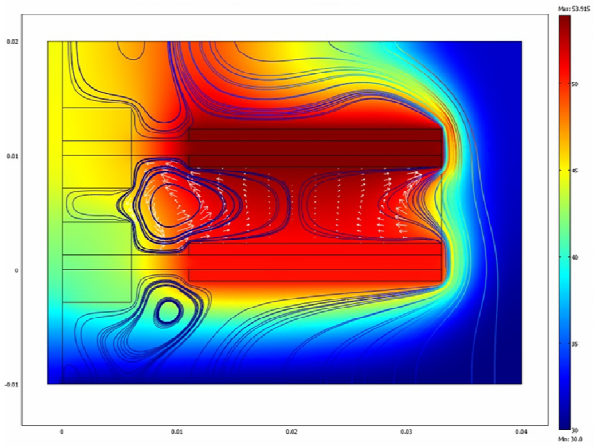

Figure 8 Thermal field and streamlines of flow at steady state.

Externally, the flow pattern is worthy influenced by flowing-up air, that sensibly modify the shape of the convective transient roll observed in the left top portion of the considered domain. On the other hand, in the left bottom volume of air, a dissipative flow structure is clearly observable. Temperature field is strongly dependent on fluid flow. The maximum detected value of velocity is about 0.095 [m/s]. Chips arranged on the top circuit board are obviously hotter than those placed on the bottom one. Maximum detected temperature is about 54 [°C] for this simulation.

Steady 3D models

Three-dimensional simulations have been carried-out for different models approximating the considered DIMM. At first we studied portions of the electronic device, delimited by transversal surfaces considered as symmetry/slipping plans. Models containing 1 and 2 chips arranged on each top surface of the overlapped PCB were firstly studied. Then more complete models have been built. In Figure 9 thermal distribution for a 8-chips model is plotted. It represents a half of a twin DIMM of 8 top-arranged chips. Lateral guides supporting PCB are observable in the left part of the simulated geometry, as well as the socket in its backside. The right transversal section surface represents the considered symmetry/slipping section of the system. Thermal and dynamical fields presented in Figure 9 and Figure 10 are obtained for a supplied power Q_{DIMM}=1 [W] and for $T_{AMBIENT}$=30 [°C].

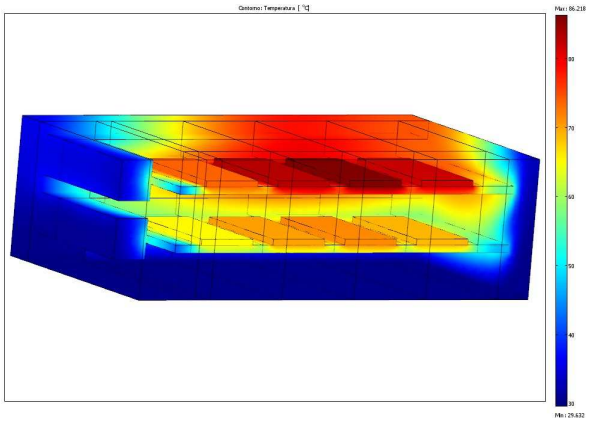

Figure 9 Temperature distribution on solid surfaces of a 8-chips model of DIMM.

Thermal distribution highlights that the maximum value of temperature is found in correspondence to the third chip placed on the top PCB. The range of the simulated operative temperatures, and the maximum detected value ($T \approx 86$ [°C]), well fit with those suggested by the leading constructors of this kind of electronic devices. The Rayleigh number (Ra) for the specific system (based on the fraction between the chip horizontal surface and its perimeter) is $Ra \in (1.1 \cdot 10^5; 1.45 \cdot 10^5)$. From Figure 10 fluid flow is observable. In that picture colour scale is plotted in order to quantify the local Nusselt number (log(Nu)). This way of plotting is helpful for emphasizing in which spatial portion of the air domain the convective heat transfer becomes preponderant with respect to the conductive heat flux. As previewed by 2D models, flow pattern principally consists in a dissipative convective roll. That thermo-convective structure is seen to assume a cylindrical shape, helicoidally developed along the backside confinement determined by the socket. From 3D simulations it is possible to observe as the convective structure also develops over lateral confinements of the fluid slot. Thermal transport direction follows the helicoidally developing of the fluid structure, from the lateral guides (left side of the Figure 10) to the lateral end-section of the geometry, where symmetry boundary conditions have been set up (right side of the Figure 10).

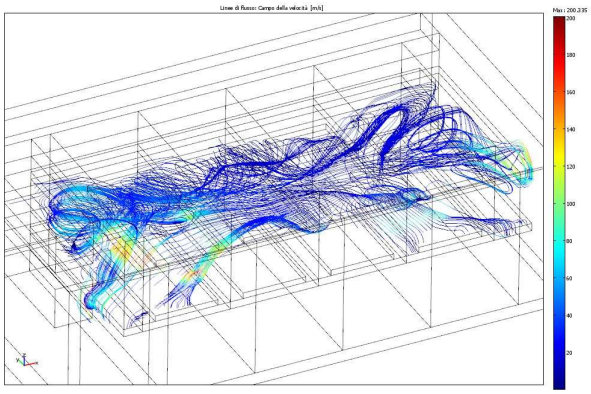

Figure 10 Streamlines of flow for a 8-chips model of a DIMM; colour scale quantifies local Nu number.

The convective eddy results more intense in the right top portion of the fluid volume, where convective heat flux reaches its maximum value. It seems that thermal energy, produced inside the control volume, is worthy transported by the highlighted roll, that "ejects" heat upward, very close to the top right corner of the fluid domain. Simulation of a system of two entire memory modules, made of two overlapped twin circuit boards, arranging 8 chips each one (for a total of 32 chips) is finally represented in Figure 11.

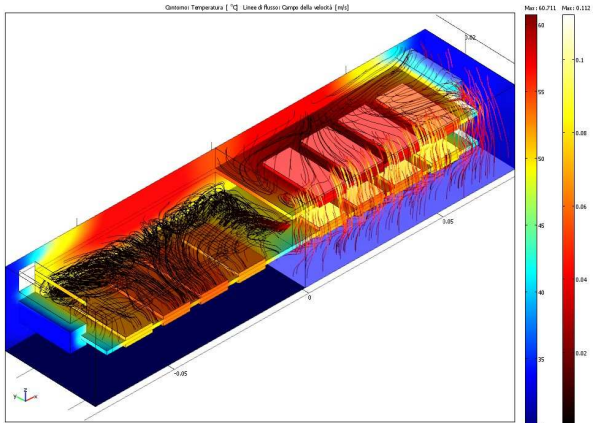

Figure 11 Temperature distribution and streamlines of flow for a double 16-chips model of DIMM obtained for $T_{AMBIENT}$=30 [°C] and Q_{DIMM}=0.5 [W] (one PCB is suppressed in plotting).

In that picture one of the four PCB is omitted in order to make clearly visible streamlines of flow in the semi-confined air volume. Both fluid-dynamical and thermal fields show coherence with results obtained for the above discussed simplified model. This means that imposition of symmetry/slipping boundary conditions at middle transversal section does not influence the physical behaviour of system. Parametric simulations as function of Q_{DIMM} and $T_{AMBIENT}$ have been carried out for the complete double DIMM model. From the obtained results a sixth order polynomial fitting law is proposed in order to correlate the maximum detected temperature with the supplied power to the DIMM and the ambient temperature. The proposed correlation equation is reported below:

$$T_{\max} = -19,5 \cdot Q_{DIMM}{}^{6} + 99,3 \cdot Q_{DIMM}{}^{5} - 204 \cdot Q_{DIMM}{}^{4} + \\ + 216,9 \cdot Q_{DIMM}{}^{3} - 132 \cdot Q_{DIMM}{}^{2} + 93,78 \cdot Q_{DIMM} + T_{AMBIENT}$$

Simulated maximum temperature values (T_{sim}) are compared with those obtained by applying the above fitting law (T_{fit}) in Table I. Reported values for $T_{AMBIENT} \in \{30; 35; 40\}$ [°C] are listed as function of $Q_{DIMM} \in (0.1; 1.2\ [0.1])$ [W]. Relative gaps between simulated and analytically evaluated temperature are also reported in Table I. As readable, the maximum gap for the studied Q_{DIMM} range of variation is 0.61 %.

Q_{DIMM}	$T_{AMBIENT}$ = 40 [°C]			$T_{AMBIENT}$ = 35 [°C]			$T_{AMBIENT}$ = 30 [°C]		
[W]	T_{sim} [°C]	T_{fit} [°C]	gap %	T_{sim} [°C]	T_{fit} [°C]	gap %	T_{sim} [°C]	T_{fit} [°C]	gap %
0.1	48.45	48.25	0.40	43.43	43.25	0.40	38.41	38.25	0.41
0.2	54.94	54.91	0.06	49.89	49.91	0.03	44.84	44.91	0.15
0.3	60.77	60.67	0.16	55.69	55.67	0.03	50.60	50.67	0.15
0.4	66.19	65.96	0.35	61.07	60.96	0.18	55.94	55.96	0.04
0.5	71.33	71.01	0.45	66.17	66.01	0.24	61.00	61.01	0.01
0.6	76.24	75.89	0.46	71.04	70.89	0.21	65.84	65.89	0.09
0.7	80.98	80.65	0.41	75.75	75.65	0.13	70.50	70.65	0.21
0.8	85.58	85.27	0.36	80.31	80.27	0.05	75.02	75.27	0.33
0.9	90.05	89.74	0.35	84.74	84.74	0.01	79.42	79.74	0.40
1.0	94.42	94.05	0.39	89.07	89.05	0.02	83.71	84.05	0.40
1.1	98.70	98.22	0.48	93.31	93.22	0.09	87.91	88.22	0.35
1.2	102.89	102.26	0.61	97.46	97.26	0.21	92.04	92.26	0.24

Table I Simulated and analytical maximum temperature values on DIMM and their relative gaps as function of ambient temperature and thermal load.

CONCLUSION

Natural convection of semi-confined air in horizontal cavities bounded by solid walls with discrete heat sources is numerically studied in the present communication. Transient and steady solutions of conservation equations are presented for 2D and 3D models. The above theoretical problem is applied to high interest technological systems exploiting that heat transfer mechanism in their operative conditions. Adopted numerical tools have been previously validated by comparison of results coming from test models with data published in literature. Results, obtained for several values of ambient temperature and supplied power to heat sources, are mainly presented in the form of temperature fields, streamlines of flow and velocity vectors. Due to semi-confinement of heated fluid, the onset of thermo-convective instability is highlighted. This manifests in arising of a complex three-dimensional flow pattern, principally consisting in a dissipative roll that helicoidally develops along lateral and backside boundaries of the considered fluid domain. That convective structure seems to significantly contribute in heat dissipation of system, transporting and ejecting thermal energy in correspondence of the frontal opened section of the semi-confined geometry. A polynomial fitting law, correlating with high precision maximum detectable temperature for studied system with ambient temperature and thermal load, is also proposed.

REFERENCES

[1] Hanreich G., Nicolics J., Musiejovsky L., High resolution thermal simulation of electronic components, *Microelectronics Reliability*, Vol. 40, 2000, pp. 2069-2076

[2] Towashiraporn P., Subbarayan G., McIlvanie B., Hunter B. C., Love D., Sullivan B., The effect of model building on the accuracy of fatigue life predictions in electronic packages, *Microelectronics Reliability*, Vol. 44, 2004, pp. 115-127

[3] El Alami M., Najam M., Semma E., Oubarra A., Penot F., Electronic components cooling by natural convection in horizontal channel with slots, *Energy Conversion and Management*, Vol. 46, 2005, pp. 2762-2772

[4] Bhowmik H., Tou K.W., Experimental study of transient natural convection heat transfer from simulated electronic chips, *Experimental Thermal and Fluid Science*, Vol. 29, 2005, pp. 485-492

[5] Harvest J., Fleischer A.S., Weinstein R.D., Modeling of thermal effects of heat generating devices in close proximity on vertically oriented printed circuit boards for thermal management applications, *International Journal of Thermal Sciences*, Vol. 46, 2007, pp. 253-261

[6] Bae H.J., Hyun J.M., Time-dependent buoyant convection in an enclosure with discrete heat sources, *International Journal of Thermal Sciences*, Vol. 43, 2004, pp. 3-11

[7] da Silva A.K., Lorenzini G., Bejan A., Distribution of heat sources in vertical open channels with natural convection, *International Journal of Heat and Mass Transfer*, Vol. 48, 2005, pp. 1462-1469

[8] Dogan A., Sivrioglu M., Baskaya S., Investigation of mixed convection heat transfer in a horizontal channel with discrete heat sources at the top and at the bottom, *International Journal of Heat and Mass Transfer*, Vol. 49, 2006, pp. 2652-2662

[9] da Silva A.K., Gosselin L., On the performance of an internally finned three-dimensional cubic enclosure in natural convection, *International Journal of Thermal Sciences*, Vol. 44, 2005, pp. 540-546

[10] Balanced Technology Extended (BTX) Interface Specification 1.0b, Intel Corporation, (2005), http://www.formfactors.org

[11] TN-47-06: Updated JEDEC DDR2 Specifications, Micron Technology Inc., 8 (2004), http://www.micron.com

[12] Technical documentation JEDEC, http://www.jedec.com

[13] TN-00-08: Thermal Applications, Micron Technology Inc., 2 (2004), http://www.micron.com

[14] Ortega A., Air Cooling of Electronics: A Personal Perspective 1981-2001, *Proceeding of the I.E.E.E. SEMITHERM Symposium*, 2002